Two Distinctive Cell Binding Patterns by Vacuolating Toxin Fused with Glutathione *S*-Transferase: One High-Affinity m1-Specific Binding and the Other Lower-Affinity Binding for Variant m Forms†

Wen-Ching Wang,* Hung-Jung Wang, and Chun-Hsien Kuo

Department of Life Science, National Tsing Hua University, Hsinchu, Taiwan

Received January 10, 2001; Revised Manuscript Received July 27, 2001

ABSTRACT: The *Helicobacter pylori* VacA causes large intracellular vacuoles in epithelial cells such as HeLa or RK13 cells. Two major VacA forms, m1 and m2, divergent in an ∼300 amino acid segment within the cell binding domain P58, display distinct cell-type specificity. Sequence analysis of four *vacA* alleles showed that a m1-like allele (61) and two m2 alleles (62 and v226) mainly differed in the midregion and that v225, a m1m2 chimera, was a natural double crossover from v226 and another allele. Each of these alleles was expressed as a soluble GST−VacA fusion that did not form a large oligomer. The recombinant VacA portion nevertheless assembled into higher ordered structures and possessed biological binding activity similar to that of the native VacA. A direct comparison of fusion-cell binding activity showed that m1 > m1m2 > m2 in HeLa cells, whereas there were more similar activities in RK13 cells. Vacuolating analyses of three forms revealed a positive correlation between cell binding activity and vacuolating activity. Moreover, the m1-type N-terminal half portion of the midregion was crucial for HeLa cell cytotoxicity. Kinetic, Scatchard, and inhibition analyses suggested the presence of at least two receptors: a m1-type specific high-affinity receptor (K_d = ∼5 nM) and a common VacA receptor interacting similarly with m1, m1m2, and m2 via a lower affinity (K_d = 45−67 nM). Expression of mainly the m1-type receptor on HeLa cells whereas both receptors on RK13 cells may account for distinct cell binding activity and therefore for cell-type specificity.

Helicobacter pylori is a Gram-negative bacterium that colonizes the stomach mucosa of ∼50% of the human population and may persist for a life-long period (*1*). It is now accepted as an essential etiologic agent for gastritis, peptic ulcer, and gastric cancer of infected patients (*2*−*4*). The *H. pylori* vacuolating toxin (VacA)[1] is a novel toxin that induces intracellular vacuoles originating from late endosomes and lysosomes in cultured eukaryotic cells (*5*−*8*). Patients infected with VacA-producing strains are more vulnerable to peptic ulceration than are those with non-VacA-producing strains (*9*). Animal studies using mice (*10*, *11*) further support that VacA is a major virulence determinant that causes the damage of gastric mucosa.

VacA shares no sequence homology with other proteins. It is synthesized as a 140 kDa polypeptide and is processed and then transported possibly via an IgA protease-like extracellular transport pathway (*12*−*14*) to yield a mature 90 kDa exotoxin, which can be further cleaved into two distinct domains, P37 and P58 (*11*, *13*, *15*, *16*). The mature exotoxin exists as an oligomeric form in neutral solution. At acidic condition, a monomeric structure is seen and VacA cytotoxicity is also activated (*17*, *18*). Sequence analysis of different *vacA* alleles shows that there are two major alleles, m1 and m2, that are divergent in an ∼300 amino acid region of P58 (they share only ∼55% amino acid identity in this region) (*9*). Distribution of these forms varies geographically; m1 type is predominant in the Central and South America (*19*) and particularly in Japan (97%) (*20*), whereas m2 form is prevalent in Taiwan (*21*) and in China (∼80%) (*22*).

Accumulated studies of VacA suggest that VacA may belong to a member of AB-type bacterial toxins and proceed to similar intoxication processes: it binds to the host cell via a B moiety, followed by internalization, translocation, and enzymatic modification of a cellular target by an enzymatically active A subunit (*23*). Given that the P37 fragment and a contiguous portion of P58 is identified as the minimal intracellular vacuolating subunit (*24*, *25*), this region may correspond to the A component. Although a cytosolic protein (VIP54) is found to interact with VacA by the yeast two-hybrid method (*26*), no enzymatic activity has been detected for VacA yet. Instead, VacA induces channel activity, allowing passage of a number of small anionic molecules (*27*, *28*), possibly via a hexameric pore seen in the lipid bilayer (*29*). Such an action may suggest a plausible mechanism for producing cellular vacuoles. It nevertheless

† This work was supported by the National Science Council (NSC 89-2320-B-007-007), Taiwan, and by the Veterans General Hospital−National Tsing Hua University−National Yang Ming University Joint Research Program (VTY88-P4-29), Medical Research Advancement Foundation in memory of Dr. Chi-Shuen Tsou, Taiwan, Republic of China.

* To whom correspondence should be addressed. Tel: 886-3-5742766. Fax: 886-3-5742766 or 886-3-5717237. E-mail: lswwc@life.nthu.edu.tw.

[1] Abbreviations: VacA, vacuolating toxin; GST, glutathione *S*-transferase; GST−VacA, fusion protein of glutathione *S*-transferase with the exotoxin polypeptide of VacA; IPTG, isopropyl β-D-1-thiogalactopyranoside; PBS, 140 mM NaCl, 2.7 mM KCl, 10 mM Na_2HPO_4, and 1.8 mM KH_2PO_4 (pH 7.3); PCR, polymerase chain reaction; SDS−PAGE, sodium dodecyl sulfate−polyacrylamide gel electrophoresis; BSA, bovine serum albumin.

10.1021/bi010065u CCC: $20.00
Published on Web 09/06/2001

cannot be excluded that VacA may possess an enzymatic activity to modify an intracellular target essential for membrane trafficking within the endomembrane system.

The other fragment of exotoxin P58 has long been considered as the B component on the basis of the observation that anti-P58 antisera block intracellular vacuolation (*30*) and that P58 from an engineered *H. pylori* strain is capable of interacting with the cell surface (*31*). Evidence of distinct cell-type specificity for m1 and m2 toxins that have polymorphic midregion sequences within the P58 domain (*9, 32*) also supports this hypothesis. By using flow cytometric analysis, a high-affinity, saturable binding pattern is indeed seen for the association of the m1 VacA with HeLa cells (*33*). In accord with this observation, there are specific cell receptors found for the m1 VacA (*34*−*36*): a 140 kDa protein on the cell surface of AZ-521, AGS and COS7 cells (*34*), 250 kDa receptor protein tyrosine phosphatase on AZ-521 cells (*35*), and epidermal growth factor receptor on HeLa cells (*36*). A further structure−function study of VacA using authentic VacA purified from *H. pylori* culture supernatants, however, is not quite feasible since only minute proteins are available. An attempt to express a soluble and functional VacA in *Escherichia coli* also failed (*37*). Recently, an alternative approach expressing a m1-type VacA fused with glutathione *S*-transferase (GST) instead was found to be able to obtain a soluble form using a very mild induction condition (*38*). The fusion nevertheless did not assemble into an oligomer normally seen for the toxin, possibly due to the N-terminal GST-tag. It also lacked vacuolating capability. Despite this, the m1 GST−VacA fusion had a binding activity similar to that of the native VacA (*38*). By characterizing several truncated fusions, the whole m1-type P58 fragment was indeed identified to be the cell binding domain in HeLa cells, confirming the previous hypothesis. Moreover, the C-terminal ∼100 amino acid segment of P58 was found to be the most crucial binding region for HeLa cells.

In this study, we sought to utilize the developed fusion approach to further investigate the role of the m1/m2 midregion sequence of VacA in cell binding activity and in cell-type specificity. We chose HeLa and RK13 cells since HeLa cells are known to be quite sensitive to the m1 toxin but insensitive to the m2 toxin, whereas RK13 cells are sensitive to both forms (*32*). Four additional *vacA* alleles (61, 62, v225, and v226) were cloned, sequenced, and used for expression: 61 was m1-like, 62 and v226 were m2, and v225 was m1m2 (*22, 39*). Each allele was successfully expressed as a GST−VacA soluble form in *E. coli*. The cell-fusion binding properties were characterized by direct measurements of fusion-cell binding intensity, kinetic, Scatchard, and inhibition analyses.

EXPERIMENTAL PROCEDURES

Materials. Buffer compounds were of analytical grade from various commercial sources. Restriction enzymes were from Promega (Madison, WI). Anti-GST mouse antibodies were from Oncogene (Boston, MA). The polyclonal rabbit anti-VacA antisera, anti-BK generated against the recombinant VacA protein consisting of 1−741 amino acids of CCUG17874, were gifts of Daniela Burroni. Fluorescein isothiocyanate-labeled anti-rabbit antibodies were from Calbiochem (San Diego, CA). Protein molecular mass standards for SDS−PAGE were from Bio-Rad (Hercules, CA).

Construction of Different VacA Forms That Fused to GST. Molecular cloning experiments were performed by standard methods (*40*). Several *vacA* alleles including 61 (m1), 62 (m2) (*22*), v225 (m1m2), and v226 (m2) (*39*) were each amplified directly from their genomic DNA and cloned into pGEM-T (Promega, Madison, WI), respectively. The nucleotide sequences of the *vacA* gene were determined for 61, 62, v225, and v226 to obtain the sequences encoding the mature polypeptide region. DNA sequencing analysis was done by the dideoxy chain termination procedure with an ABI Prism Dye Terminator Cycle Sequencing Ready Reaction Kit (Perkin-Elmer-Cetus, Perkin-Elmer Corp., Norwalk, CT) in an automated DNA sequencer (model 377-96; Perkin-Elmer-Cetus, Perkin-Elmer Corp., Norwalk, CT). Sequence analysis was done with the University of Wisconsin Genetics Computer Group (Madison, WI) package. For preparation of a plasmid encoding the GST−VacA protein, a *vacA* fragment encoding the mature exotoxin was created by polymerase chain reaction (PCR) using the following oligonucleotides as primers: W-F (5′CGGGATCCGCCTTC-TTTACAACCGTGATC3′) and W-R (5′GCGCTCGAGT-TAGAGAGCGTAGCTAGCGAAACG3′). The primers used for PCR introduced a *Bam*HI site (underlined) at the 5′ end and a *Xho*I site (underlined) in the 3′ end. The *Bam*HI−*Xho*I fragment was then cloned into the *Bam*HI and *Xho*I sites of the polylinker of the expression vector pGEX 4T-1 (Pharmacia Biotech, Piscataway, NJ) to obtain the GST−VacA construct. The insert was verified by sequencing analysis.

Purification of Native Toxins and GST−VacA Fusions. H. Pylori 60190 (ATCC 49503) (*9*), v225 and v226, after being grown on blood agar plates (*41*), was cultured in brucellar broth containing 0.2% β-cyclodextrin for 2−3 days in a controlled microaerophilic atmosphere. Fermentor facilities were used for volumes larger than 1 L. VacA was purified from the broth culture supernatants according to Cover et al. (*42*). Expression of the GST−VacA fusion in *E. coli* BL21(DE3) cells carrying the recombinant plasmids (OD_{600nm} = 0.8) was induced by 0.02 mM IPTG at 20 °C for 16 h (*38*). Bacterial pellets were fractionated, and soluble proteins in cytosolic fractions were collected and purified through glutathione−Sepharose 4B affinity chromatography according to the protocol suggested by the supplier (Pharmacia Biotech, Piscataway, NJ). Protein concentrations were determined using the BCA protein assay (Pierce, Rockford, IL). VacA concentrations were additionally determined by SDS−PAGE analysis, followed by densitometric scanning (computing densitometer 300E; Molecular Dynamics, Sunnyvale, CA), and then calculated on the basis of a molecular mass of 87 kDa. Fusion concentrations were calculated on the basis of a molecular mass of 110 kDa.

Glycerol Density Gradient Centrifugation. Samples of the fusion or the cleaved fusion by thrombin were layered on 3 mL 15−40% glycerol gradients prepared in 100 mM NaCl containing 60 mM Tris, pH 7.5, and centrifuged at 30000 rpm for 8 h in an RPS56T-267 rotor (Hitachi, Tokyo, Japan). Fractions (100 μL) from the tops of the gradients were collected and analyzed by 7.5% SDS−PAGE and immunoblotting with anti-VacA antisera. Standards including bovine serum albumin (4.6 S), catalase (11.2 S), and urease (18.6 S) were fractionated in parallel gradients.

Vacuolating Cytotoxin Assay. Vacuolating activity was assessed using the in vitro HeLa or RK13 cell assays, as previously described (*22*, *32*). HeLa cells were cultured in Dulbecco's modified minimal essential medium containing 10% fetal bovine serum. RK13 cells were grown in α minimal essential medium containing 10% fetal bovine serum. To quantify the vacuolating activity, the uptake of neutral red into the vacuoles of the VacA-treated cells was measured according to Cover et al. (*43*).

Flow Cytometric Analysis. The monolayer cells were detached by the treatment of the EDTA solution (1 mM EDTA in PBS) or by the trypsin−EDTA solution (0.01% trypsin and 0.53 mM EDTA in PBS). Cells (10^5) were incubated with GST−VacA or GST diluted in PBS containing 3% bovine serum albumin (BSA) at 4 °C for 1 h. After three washes with cold PBS containing 3% BSA, cells were fixed with 2% paraformaldehyde. Cells were then incubated with anti-GST (10 μg/mL) (Oncogene, Boston, MA) or anti-VacA antiserum (1:1000) at 4 °C for 30 min. Cells were washed three times in cold PBS−BSA and then incubated with fluorescein isothiocyanate-labeled anti-rabbit IgG (1:250) (Calbiochem, San Diego, CA) at 4 °C for 30 min. Cells were washed and resuspended in 500 μL of 1% paraformaldehyde. Flow cytometric analyses were carried out on a FACScan flow cytometer (Becton Dickinson, Los Angeles, CA). To correct for nonspecific association from GST, the mean fluorescence intensity (MFI) value from each of the experiments with the anti-GST antisera was subtracted from the value obtained for cells incubated with GST only. For blocking experiments, 10^5 cells were incubated in the fresh medium containing 2% fetal bovine serum with a fusion (10 nM) alone or plus 1 μM m1, m2, or both native toxins at 4 °C for 12 h, followed by similar staining and flow cytometric analysis procedures. For kinetic experiments, 10^5 cells were incubated in the fresh medium containing 2% fetal bovine serum with a fusion (10 nM) alone or plus 1 μM corresponding native toxin at 4 °C for the times indicated. For Scatchard experiments, 10^5 cells were incubated with various concentrations of a fusion alone or plus a 100-fold molar excess of its corresponding native toxin at 4 °C for 12 h. To examine whether a native toxin was a true competitive inhibitor, 10^5 cells were incubated in the fresh medium containing 2% fetal bovine serum with various concentrations of a fusion plus various fixed concentrations of a native toxin at 4 °C for 12 h. Cells were stained, followed by flow cytometric analysis as above.

Western Blotting. After SDS−PAGE, proteins were transferred onto nitrocellulose membranes (Hybond-C extra, 0.45 μm; Amersham, Uppsala, Sweden). The blots were incubated with the anti-VacA antibody (1:5000) and then with peroxidase-conjugated goat anti-rabbit antibody (1:2000). The proteins were detected using the enhanced chemiluminescence (ECL) system (Amersham, Uppsala, Sweden).

Nucleotide Sequence Accession Numbers. The nucleotide sequences were deposited in GenBank under accession numbers AF195011−AF195012 and AF291094−AF291095.

RESULTS

Sequence Analysis of vacA Alleles from m1, m2, and m1m2 Strains. We took advantage of utilizing *vacA* alleles from Taiwanese isolates including a m1-like strain, 61, and a m2 strain, 62. In addition, two strains, v225 and v226, which were from a single patient and had 324 bp identical sequences in an aligned 0.64 kb *vacA* midregion (*39*), were chosen in this investigation. Sequences encoding the mature exotoxin for these four alleles were determined. Analysis of the aligned region (34−859 residues of 60190) between 61 (m1) and 62 (m2) revealed that 61 and 62 had a highly conserved P37 subunit (99% identity in the 34−326 residues of 60190) but a markedly divergent P58 cell binding subunit (69% identity in the 327−859 residues of 60190). For v226, it had a high homology with strain 62 (96% amino acid identity) and belonged to a member of the m2 family. For v225, we found that v225 and v226 had essentially identical sequences except in the N-terminal half portion of the middle region (corresponding to 488−640 residues of 60190) (Figure 1A). In this region, they shared only 55.6% amino acid identity, confirming that v225 was a m1m2 chimeric allele. Given the genetic similarity between v225 and v226, v225 should

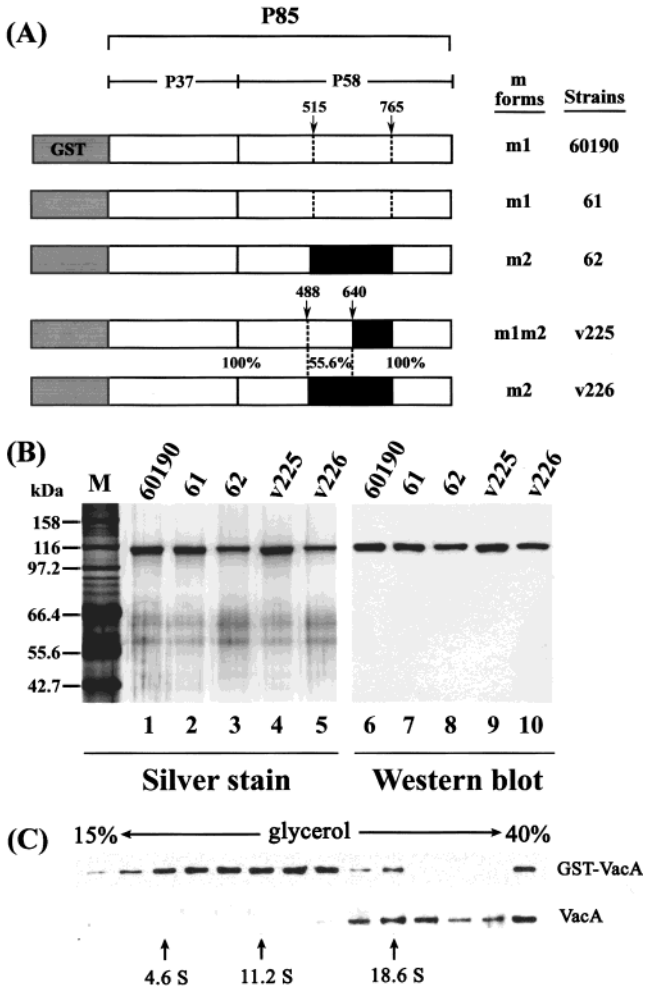

FIGURE 1: Expression of different m forms that fused with GST. Panel A: Schematic representation of different m fusions. Panel B: SDS−PAGE (lanes 1−5) analysis of the purified fusions and Western blot (lanes 6−10) analysis of the purified fusions by anti-BK antibody. Lanes: 1 and 6, 60190; 2 and 7, 61; 3 and 8, 62; 4 and 9, v225; 5 and 10, v226. Panel C: Glycerol gradient sedimentation of GST−VacA or the cleaved VacA portion after thrombin digestion at neutral pH. Samples were prepared and centrifuged as described under Experimental Procedures. VacA was detected by immunoblotting with anti-VacA antibody and enhanced chemiluminescence reagents. The positions of standards sedimented in a parallel gradient are shown at the bottom [bovine serum albumin (4.6 S), catalase (11.2 S), and urease (18.6 S)].

be a natural double crossover offspring from v225 and another parent allele.

GST−VacA Expression, Purification, and Characterization. To characterize the binding properties of variant m forms fused with GST, expression plasmids harboring genes encoding the mature VacA exotoxin were constructed (Figure 1A). All fusion proteins were expressed by an induction condition (0.02 mM IPTG at 20 °C for 16 h) as previously described (*38*). After passage over an affinity chromatography column using a glutathione−Sepharose matrix, a major band of an apparent molecular mass of ∼110 kDa was observed in the soluble fractions (Figure 1B). Each of these 110 kDa proteins was recognized by the anti-VacA antibody (Figure 1B), thus indicating that the 110 kDa protein was the GST−VacA fusion. Approximately 0.2 mg of pure protein per liter harvest was obtained. We have previously shown that the fusion could not form an oligomer normally found for native VacA possibly because of the additional GST domain (*38*). To further assess whether the VacA portion of the soluble GST−VacA could reassemble into an oligomer, the fusion was digested by thrombin and the derived VacA portion was then analyzed by velocity sedimentation on glycerol density gradients. As shown in Figure 1C, the recombinant 60190 VacA assembled into an oligomeric state (∼22 S) like that of the native VacA in neutral solution, as compared with ∼8 S seen for the fusion (*38*). We also determined whether a recombinant VacA could block its corresponding fusion-cell association. The cell binding analysis was conducted for each fusion alone or plus a 100-fold molar excess of its corresponding recombinant or native toxin. As expected, there were nearly identical blocking effects for the recombinant VacA and native VacA (data not shown).

Vacuolating Activity of Variant m Toxins on HeLa and RK13 Cells. VacA was purified from culture supernatants of 60190, v225, and v226, respectively (Figure 2A). Purified VacA was then assessed for vacuolating activity in HeLa cells. As shown in Figure 2B, 60190 native toxin (m1) produced higher vacuolating activity than did v225 (m1m2) ($P < 0.05$) and than did v226 (m2) ($P < 0.005$) in HeLa cells. The m2 toxin (v226) had nearly no toxicity, as expected. For the 60190 fusion, no activity was detected (Figure 2B), possibly because of the presence of an additional GST domain in the N-terminal end of VacA (*24*, *25*). The vacuolating activity for RK13 cells was also determined. As seen in Figure 2C, all three native toxins induced neutral red uptake in RK13 cells, and the level of vacuolating activity was m1 > m1m2 ≥ m2 as compared with none for the 60190 fusion molecule. It was nevertheless noted that v225 (m1m2) and v226 (m2) had rather similar vacuolating phenotypes in RK13 cells.

HeLa and RK13 Cell Binding by Variant m Fusions. The binding of the m1, m2, or chimeric fusion to HeLa cells was first characterized at 4 °C for 1 h by flow cytometric analysis as previously described (*38*). The binding of various m forms increased as a function of concentration and finally reached a plateau at ∼100 nM (*38*), and the level of binding was found to be m1 (61, 60190) > m1m2 (v225) > m2 (v226, 62) (data not shown). Interstrain variation of cell association was seen between the two m1 fusions and between the two m2 fusions, respectively, reflecting their interstrain genetic heterogeneity in VacA. For RK13 cells, despite that the pattern was also m1 > m1m2 > m2, there were more comparable binding affinities among variant m forms (data not shown). Cell preparations by either the trypsin-based or the EDTA-treated method gave similar binding activities in HeLa or RK13 cells (data not shown).

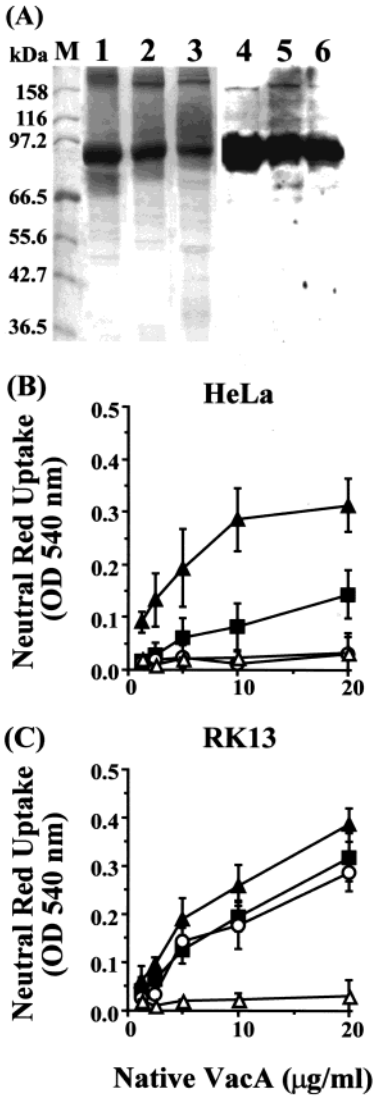

FIGURE 2: Vacuolating activity of the m1, m1m2, or m2 VacA. Panel A: SDS−PAGE (lanes 1−3) and Western blot (lanes 4−6) analyses of the purified VacAs. Lanes: 1 and 4, 60190; 2 and 5, v225; 3 and 6, v226. Panels B and C: Vacuolating activity of purified VacA from 60190 (▲), v225 (■), or v226 (○) or the 60190 fusion (△) on HeLa cells (panel B) or on RK13 cells (panel C) as determined by the neutral red uptake assay.

The two m native toxins were examined as inhibitors of the fusion-cell association. In the presence of a 100-fold molar excess of native m1 VacA (60190) in HeLa cells at 4 °C for 12 h, the binding of the 60190 fusion was reduced from 100% to ∼10%. On the other hand, the percent of MFI was reduced to 79% in the presence of a 100-fold molar excess of native m2 VacA (v226) (Table 1). Similar results were also obtained in RK13 cells, thus indicating that the m1 fusion-cell association was blocked strongly by native m1 toxin but weakly by m2 toxin in either of the two cells. For the inhibition of the m2 fusion (v226)-cell association, the native m1 and m2 VacAs had similar blocking capabilities in RK13 cells: the association was reduced from 92% to ∼55% by either of the two native toxins. For HeLa cells,

Table 1: Inhibition of Fusion-Cell Association by Variant Native VacAs

	percent of binding (% of MFI)[a]					
	HeLa + GST−VacA[b]			RK13 + GST−VacA[b]		
inhibitor	60190 (m1)	v226 (m2)	v225 (m1m2)	60190 (m1)	v226 (m2)	v225 (m1m2)
no[c]	100.0 ± 11.1	42.4 ± 5.8	80.6 ± 11.4	125.7 ± 8.9	91.8 ± 8.8	92.0 ± 8.1
60190 (m1)[d]	10.3 ± 2.3	34.7 ± 4.6	19.8 ± 5.7	28.3 ± 4.9	57.4 ± 3.2	37.7 ± 6.1
v226 (m2)[d]	78.9 ± 5.8	35.1 ± 5.8	58.1 ± 9.8	97.0 ± 6.6	50.1 ± 3.2	41.8 ± 7.1
60190[d] + v226[d]	11.1 ± 1.3	27.3 ± 6.7	19.3 ± 5.7	29.0 ± 7.3	34.5 ± 4.6	27.2 ± 6.6
v225 (m1m2)[d]	−[e]	−	15.9 ± 4.5	−	−	20.0 ± 4.6

[a] To normalize the data, each value was calculated as the percentage of the MFI obtained for the 60190 fusion-HeLa cell association in the absence of competitor. [b] HeLa or RK13 cells (10^5) were incubated in the fresh medium containing 2% fetal bovine serum with 10 nM GST−VacA fusion in the absence or presence of competitor. [c] No competitor was added. [d] Final concentration, 1 μM. [e] Not determined.

there was a similar blocking pattern despite the relatively low binding. We also determined the inhibition of the chimeric fusion-cell association. As seen in Table 1, the blocking pattern was more similar to that of m1 fusion-cell association in HeLa cells: both m1 and m1m2 toxins strongly blocked the binding, whereas the native m2 toxin had much weaker inhibiting capability. In RK13 cells, by contrast, the chimeric-cell association was blocked approximately equally by either m1 or m2 native toxin. A comparison between the presence and the absence of the native toxin with each of the fusions revealed that the specific association was m1 (61, 60190) > m1m2 (v225) > m2 (v226, 62) in HeLa cells. In RK13 cells, despite that the pattern was also m1 > m1m2 > m2, there were more comparable activities, particularly between v225 and v226. It was also noted that the m2 fusion had much higher specific binding in RK13 cells and that there was nearly no specific binding for the m2 fusion in HeLa cells.

Analysis of a fusion-cell binding level (Table 1) versus the vacuolating activity of its corresponding native toxin (Figure 2B,C) indicated that there was a positive correlation. It was particularly noted that (i) for the m1 type, it had the highest specific binding activity and vacuolating activity in both cells, (ii) for the m2 form, there was nearly no specific association and vacuolating activity in HeLa cells, whereas higher specific binding and vacuolating activity was seen in RK13 cells, and (iii) for two closely related forms, v225 (m1m2) and v226 (m2), binding and vacuolating activities were nearly identical in RK13 cells but quite different in HeLa cells. These results strongly suggested that the m1-type midregion, particularly the m1-type N-terminal half portion of the midregion, was essential for HeLa cell binding activity as well as vacuolating activity. In addition, a higher VacA binding activity resulted in a higher vacuolating activity, suggesting that expression of specific receptors on the cell surface might serve as a basis for distinct binding activity and therefore for different cell-type specificity. On the basis of the above results, we propose that (i) in HeLa cells, there may be a m1-type specific receptor *RM*1, and (ii) in RK13 cells, there may be a common receptor (*RMX*) that interacts similarly with variant m forms. Alternatively, there may be both m1-type (*RM1*) and m2-type (*RM2*) receptors present on the cell surface of RK13 cells. Other combinations such as *RM1* plus *RMX* or *RM2* plus *RMX* or more than two receptors on RK13 cells are also possible. To test these possibilities, kinetic and Scatchard analyses along with various competition experiments were thus conducted as in the following.

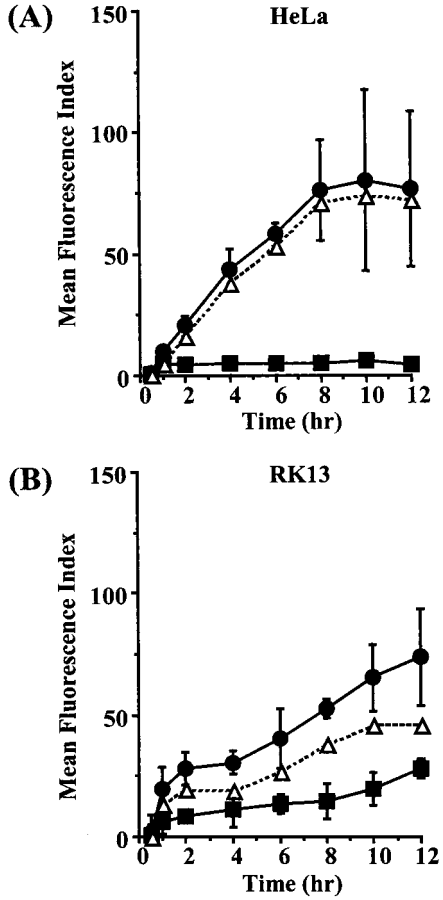

FIGURE 3: Kinetic analysis of fusion-cell association. Panel A: HeLa cells were incubated in the fresh medium, 2% fetal bovine serum with the 60190 fusion (10 nM) alone or plus a 100-fold molar excess of the native 60190 toxin (1 μM). Panel B: RK13 cells were incubated in the fresh medium, 2% fetal bovine serum with the v226 fusion (10 nM) alone or plus a 100-fold molar excess of the native v226 toxin (1 μM). At the times indicated, triplicate samples were processed and analyzed by flow cytometry (see Experimental Procedures). Symbols: (●) fusion; (■) fusion + native toxin; (△) difference between (●) and (■).

Kinetic Analysis. Figure 3A shows the kinetics of the m1 fusion−HeLa cell association at 4 °C. The level of association increased with time and reached a steady state after 8 h. In the presence of a 100-fold excess of native VacA, association was still observed, but its magnitude was considerably reduced. The intensity shift observed here was thus considered as nonspecific binding. The difference between association of the m1 fusion in the absence and presence of native m1 toxin was subsequently referred to as

specific association. After calculation, specific association followed the similar pattern as association of the m1 fusion alone and approached >90% of the total at the final steady state. Similar results were also obtained for of the m1 fusion in RK13 cells (data not shown). For the m2 fusion, kinetic analysis and the following experiments were only determined for RK13 cells due to its low binding intensity in HeLa cells. As shown in Figure 3B, there was also a saturable time−course curve, and the specific association reached a plateau after 10 h at 4 °C. Cell preparations by either the trypsin-based or the EDTA-treated method yielded similar results (data not shown). The level of the m2 fusion−RK13 cell association was, nevertheless, lower than that of the m1 fusion-cell association. We also compared the cell binding kinetics between a fusion (m1 or m2) and its corresponding recombinant VacA portion using anti-VacA antisera. It appears that both proteins had similar binding kinetic curves (data not shown), thus further supporting the biological significance of the recombinant VacA.

Scatchard Analysis. As shown in Figure 4A, the effect of the m1 fusion (60190) concentration (range from 0.1 to 220 nM) on the level of specific association was assessed by a parallel incubation in which a 100-fold excess of native 60190 VacA was added. The specific association in RK13 cells increased as a function of GST−VacA up to about 100 nM where saturation was achieved. By use of the method of Scatchard, a nonlinear line was obtained in RK13 cells (inset in Figure 4A), indicating that there might be non-equivalent binding sites for the m1 fusion. Similar results (a nonlinear line) were also obtained for the binding kinetics of the m1 fusion in HeLa cells (data not shown). For the m2 fusion, the effect of the v226 fusion concentration on the level of specific association was also determined for RK13 cells (Figure 4B). Contrary to that seen for the m1 fusion, Scatchard plot analysis revealed a linear line (inset in Figure 4B) and an estimated K_d of 46 nM was obtained, indicating that there were equivalent binding sites for the m2 fusion in RK13 cells.

Inhibition of Fusion-Cell Binding by Variant Native Toxins. To examine whether the m1 native toxin was a true competitive inhibitor against the m1 fusion binding, RK13 cells were treated with the m1 fusion plus increasing fixed concentrations of the native 60190 toxin (range from 0 to 5 nM), followed by cell staining and flow cytometric analysis. Lineweaver−Burk analysis demonstrated that the m1 native toxin exhibited simple competitive inhibition against the m1 fusion (Figure 5A). The lines at various fixed concentrations of native toxin intersect at the 1/MFI axis, indicating that the native toxin can be competed away at high GST−VacA concentrations, consistent with the results in Table 1. Moreover, the lack of a 1/MFI−intercept effect indicated that the m1 native toxin and the m1 fusion both bound to the same receptor. By replotting each slope versus the corresponding inhibitor concentration at which it was obtained, an inhibition constant of about 4 nM was derived (inset in Figure 5A). Similar results were also obtained for HeLa cells in which the m1 native toxin was also a competitive inhibitor against the m1 fusion (data not shown) and an inhibition constant of about 5 nM was derived.

For the inhibition of the m2 fusion-cell association, RK13 cells were treated with the v226 fusion plus increasing concentrations of the native v226 toxin (range from 0 to 160 nM), followed by cell staining and flow cytometric analysis. Lineweaver−Burk analysis showed that the m2 native toxin reduction of fluorescence intensity followed the binding kinetics of a true competitive inhibitor (Figure 5B). An inhibition constant of about 67 nM was obtained (inset of Figure 5B) as compared with K_d of 46 nM calculated from Scatchard analysis (Figure 4B). For the m1 native toxin, it also displayed simple competitive inhibition against the m2 fusion in RK13 cell binding (Figure 5C), with an inhibition constant of about 45 nM (inset in Figure 5C). Given the relatively small difference in the values seen between K_d and K_i, the GST domain of the fusion would contribute little to the binding energy, thus hardly participating in cell binding activity. Moreover, the similar inhibiting patterns seen in panels B and C of Figure 5 indicated that the native m1 and

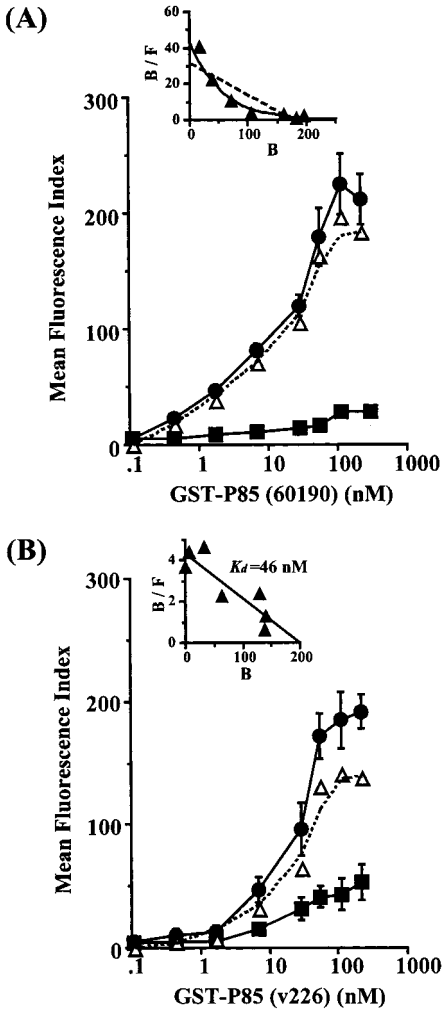

FIGURE 4: Scatchard analysis of fusion-cell association. RK13 cells (10^5) were incubated in the fresh medium, 2% fetal bovine serum with either the m1 fusion (60190) alone or plus a 100-fold molar excess of the 60190 native toxin (three replicates) at 4 °C for 12 h (panel A). RK13 cells (10^5) were incubated in the fresh medium, 2% fetal bovine serum with either the m2 fusion (v226) alone or plus a 100-fold molar excess of the v226 native toxin (three replicates) at 4 °C for 12 h (panel B). The experiments were performed in triplicate. Fusion-cell binding intensity was then measured as described in Experimental Procedures. Symbols: (●) fusion; (■) fusion + native toxin; (△) difference between (●) and (■). The inset in each panel shows the Scatchard plot of the specific cell-associated MFI. Bound MFI (*B*) is plotted on the abscissa and bound/free (*B*/*F*) on the ordinate. The line was fitted by regression analysis.

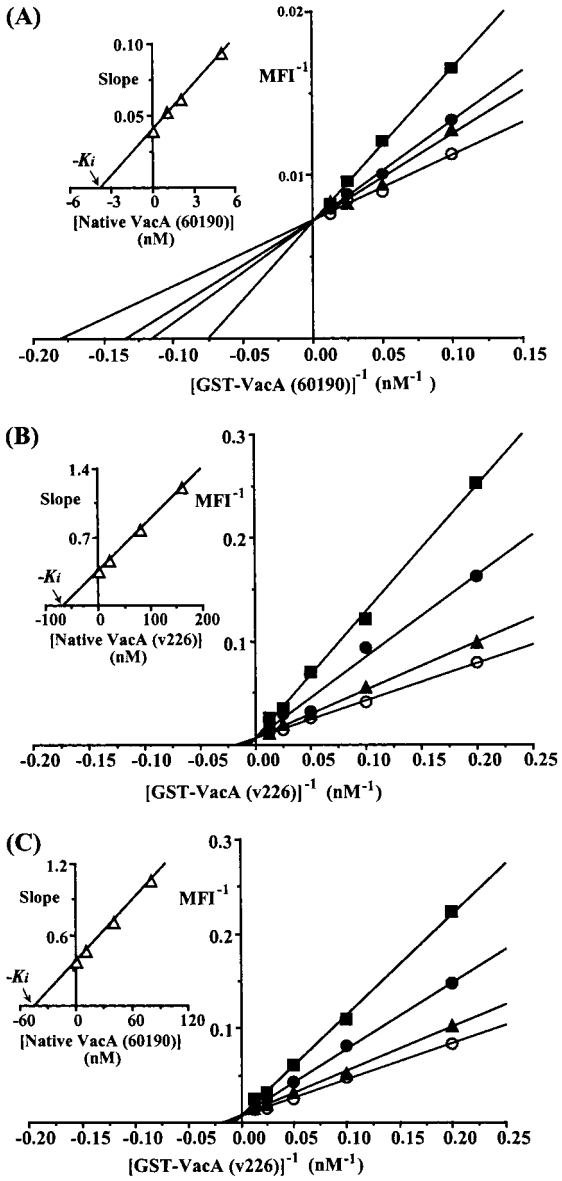

FIGURE 5: Inhibition of fusion-cell association by native VacA. RK13 cells (10^5) were incubated in the fresh medium, 2% fetal bovine serum with the m1 fusion (60190) plus various fixed concentrations of the native 60190 toxin (■, 5 nM; ●, 2 nM; ▲, 1 nM; ○, 0 nM) at 4 °C for 12 h (panel A). RK13 cells (10^5) were incubated with the m2 fusion (v226) plus various fixed concentrations of the native v226 VacA (panel B: ■, 160 nM; ●, 80 nM; ▲, 20 nM; ○, 0 nM) or the native 60190 VacA (panel C: ■, 80 nM; ●, 40 nM; ▲, 10 nM; ○, 0 nM) at 4 °C for 12 h. The experiments were performed in triplicate. Fusion-cell binding intensity was then measured as described in Experimental Procedures. Data are presented in double reciprocal form, where 1/MFI is plotted versus 1/[fusion], at various fixed concentrations of the native toxin. The inset in each panel shows the slope versus [native VacA].

m2 toxins exerted similarly competitive inhibiting effects on the m2 fusion−RK13 cell binding, consistent with the results in Table 1. The lack of a 1/MFI−intercept effect further suggested that the m1 and m2 native toxins and the m2 fusion bound to the same receptor.

DISCUSSION

In this study, different m alleles including m1 (61), m2 (62 and v226), and an unusual chimera m1m2 (v225) were cloned and used for expression in *E. coli*. Sequence analysis of these alleles confirmed previous results in which there was high homology (>95%) among each of the m1 and m2 groups, respectively, whereas a m1 strain was less homologous to a m2 strain mainly because of the divergent ~300 amino acid region within P58 (*9*). The finding that v225 (m1Tm2) and v226 (m2) had essentially identical exotoxin sequence except in a 152-residue region (corresponding to the N-terminal half portion of the divergent middle region) and that v225 and v226 were colonized in the same patient (*39*) suggested that v225 was a natural double crossover offspring from v226 and another parent allele. These results also supported the frequent recombination seen for *H. pylori* (*39*).

Each of these alleles was successfully expressed as a soluble GST−VacA fusion by using a very mild induction condition (*38*). We have previously shown that a soluble m1 fusion possessed several properties related to the native VacA: (i) a conformational sensitive monoclonal antibody C1G9 could recognize the m1 fusion, (ii) the fusion blocked the vacuolating activity induced by the native toxin, and (iii) the fusion had a binding affinity similar to that of the native VacA (*38*). Although the fusion did not form a large oligomer normally found for native VacA (*38*), we showed that the recombinant VacA without the GST-tag indeed assembled into a higher ordered structure in neutral solution. Moreover, the VacA portion could successfully block the fusion-cell association. These results collectively suggest that the recombinant VacA folds into a tertiary structure virtually identical with that of native VacA. In addition, the fusion binds to cells in a manner similar to that of the multimeric recombinant VacA, in agreement with the fact that the crucial C-terminal binding segment in P58 is distant from the GST-tag (*38*). Another advantage of using GST−VacA is its common GST-tag, enabling a direct comparison of the cell binding activities among variant m fusions, as opposed to the difficulty seen for native VacA because of the lack of an appropriate antibody recognizing the same epitope of various VacAs (*32*). Subsequent binding experiments were thus investigated with GST−VacA that was locked into a predominantly monomeric state. We showed that the level of binding activity was m1 > m1m2 > m2 in HeLa cells, whereas there were more similar activities among these forms in RK13 cells. Analysis of vacuolating activity also showed that m1 > m1m2 > m2 in HeLa cells, whereas there were more comparable activities in RK13 cells. For each form, there was a positive correlation between the binding activity and the vacuolating activity. It was particularly noted that the two closely related forms, v225 (m1m2) and v226 (m2) that had only a 152-residue difference in the N-terminal half portion of the middle region, exerted their effects similarly on RK13 cells. However, for HeLa cells, there was much higher activity for v225 than for v226. Of interest, related observations in vacuolating phenotypes of a natural and several engineered *H. pylori* chimeras were also reported in a recent publication (*44*). They showed that the first N-terminal 35 amino acids of the middle region must be m1-type for HeLa cell cytotoxicity, whereas all chimeric proteins tested were fully toxic to RK13 cells, despite the lack of evidence of binding activity. Taken together, these data suggest that VacA binding activity is a major factor for vacuolating activity.

To examine whether there are specific receptors on HeLa and RK13 cells, binding analyses analogous to the classical receptor−radioligand experiments were conducted. A high-affinity, specific, saturable binding pattern was indeed observed for the m1 fusion in either HeLa or RK13 cells. Additional lines of evidence further supported the presence of a specific, high-affinity m1-type receptor, *RM1*: (i) other reports also presented that the m1 native toxin displayed a high-affinity binding pattern in HeLa cells (*32*, *33*) or in RK13 cells (*32*), (ii) several high-affinity m1 VacA associated proteins are identified (*34*−*36*), (iii) as presented in this investigation, the m1 fusion-cell association was strongly inhibited by the native m1 toxin but weakly by the native m2 toxin in either HeLa or RK13 cells, and (iv) the m1 native toxin reduction of the m1 fusion-cell fluorescence intensity followed the binding kinetics of a true competitive inhibitor in either of the two cell lines and had similar K_i values (HeLa cells, $K_i = 5$ nM; RK13 cells, $K_i = 4$ nM). These data thus suggest the presence of a m1-type receptor (*RM1*) not only on HeLa but also on RK13 cells that can interact specifically with the m1 VacA. On the basis of the difference seen between v225 and v226 in HeLa cells, *RM1* is also expected to be highly specific to the m1-type VacA in which the N-terminal half portion (515−765 amino acids) of the middle region should correspond to the m1 sequence. In addition, given that the m1 fusion binding was strongly blocked by the m1 native toxin, the GST portion of the m1 fusion should contribute little to bind to *RM1*. Thus, the dissociation constant for the m1 toxin and *RM1* interaction would then be approximately equal to that of K_i, i.e., $K_d = \sim 5$ nM, confirming a high-affinity, specific bimolecular binding.

Two recent reports, however, failed to show a specific binding manner for the m1-type VacA by utilizing the classical iodinated ligand binding method (*45*, *46*). Examination of the binding assays in these studies reveals two main differences. First, as presented here, a steady state was only reached after 8 h for the m1 fusion-cell association and a saturable binding was observed at rather high concentration of GST−VacA (∼100 nM). In contrast, much less incubation time and much lower toxin concentration were used in the other studies, which might account in part for why there were lower affinity, nonsaturable binding responses. Second, while they utilized the acid-treated ^{125}I-labeled native VacA as a ligand (*45*, *46*), we used the GST−VacA fusion in this study. Based on the fact that the radioactive VacA retains vacuolating activity (*45*, *46*), it is conceivable that the labeled ligand would be able to complete the whole intoxication process as proposed by Reyrat et al. (*47*): (i) the toxin first interacts with its primary cell-surface receptor, possibly via its P58 subunit, (ii) active monomeric toxin then inserts into the plasma membrane that requires P37 domain, and (iii) there are subsequent actions including internalization that requires active cellular process (*45*) and the formation of anion-selective channels. Furthermore, the treatment of ligand with acid not only allows dissociation of oligomers but also causes other structural alterations (*17*), which may lead to interact with other cell-surface components (*35*, *46*) for subsequent cytotoxic processes and then to facilitate vacuolating activity (*17*, *18*). In accordance with this model, McClain et al. (*45*) indeed observed several iodinated VacA fragments protected from proteolysis after binding with cells at 4 °C, indicating the possibility that the activated ^{125}I ligand might progress from stage i into stage ii and insert into the plasma membrane. In this case, acid-activated ^{125}I VacA would then hardly be competed with excess unlabeled VacA, which provides another plausible interpretation for why there is a high level of noncompetable binding. On the other hand, the soluble fusion consists of an additional N-terminal GST domain and cannot induce vacuolation, although it possesses cell binding activity similar to that of the native VacA. Given that P37, particularly the region close to the N-terminal end, is critical for vacuolating activity (*48*), the N-terminal P37-linked GST-tag of the soluble fusion is speculated to prevent GST−VacA from progressing into subsequent intoxication processes such as membrane insertion after binding to cells. Fusion molecules may then largely remain in the primary binding stage and interact with the primary receptor via a reversible, bimolecular reaction, allowing an effective competition by excess native VacA as seen in the present study.

The finding of several potential m1-type receptors on various cell lines (*34*−*36*) may first seem to imply that different cell lines possess distinct *RM1*. However, two proteins (a 140 kDa protein and 250 kDa receptor protein tyrosine phosphatase) are found to both co-immunoprecipitate with VacA (*34*, *35*) on AZ-521 cells. One interpretation is that these proteins are both authentic VacA receptors as *RM1* or *RMX* for RK13 cells (see below). Alternatively, some may not serve as the primary VacA receptors. Ricci et al. recently reported that a highly m1-type sensitive cell line, HEp-2, after removing glycosylphosphatidylinositol (GPI) anchored proteins from the cell surface, becomes barely susceptible to VacA without losing VacA binding activity (*46*), indeed implicating the presence of other VacA-associated cell-surface proteins for high cell sensitivity to VacA. Whether *RM1* represents the same molecule between HeLa and RK13 cells nonetheless requires additional investigation.

For the m2 fusion, a saturable response was also seen in RK13 cells, despite the lower specific binding intensity. In addition, a linear line on the Scatchard plot was observed, and a dissociation constant of 46 nM was derived. These results thus suggest the presence of a specific receptor, *RM2*, for the m2 fusion on RK13 cells. Since the m2 fusion−RK13 cell association was blocked similarly by either native m1 or m2 toxin (Table 1) and since either of the two native toxins was a true competitive inhibitor (Figure 5), it seemed likely that *RM2* interacted approximately equally with both forms. The finding that the two K_i values (the native m1 toxin as an inhibitor, 45 nM; the native m2 toxin as an inhibitor, 67 nM) were quite close to the K_d value (46 nM) further supported this possibility. Thus, *RM2* is reconsidered as *RMX* that can interact similarly with different m forms via a dissociation constant of about 45−67 nM.

On the basis of the above discussions, at least two receptors, *RM1* and *RMX*, would be present on the cell surface of RK13 cells to associate with the m1 form. The finding that VacA interacts with lipid membrane (*29*, *49*) may provide additional lower affinity interactions. A portion of binding sites are therefore of high affinity (*RM1*, $K_d = \sim 5$ nM), whereas some are of low affinity (*RMX*, $K_d = 45\sim67$ nM) or close to nonspecific interactions, resulting in the nonlinear curve of the m1 fusion−RK13 cell binding seen in the Scatchard plot. Similarly for HeLa cells, there may be multiple receptors to associate with the m1 fusion, as suggested in the Scatchard analysis. However, since the

m1 form yielded the highest binding and since there was very low binding for the m2 form, *RM1* is expected to be the major VacA receptor on HeLa cells, in accord with our previous prediction. A predominant bimolecular, m1-specific, high-affinity reaction for VacA binding in HeLa cells is thus expressed as $RM1 + M1 \leftrightarrow RM1{\cdot}M1$ via $K_d = \sim 5$ nM. Results from the chimerical fusion−HeLa cell binding experiments also supported this model.

In conclusion, sequence analysis of four *vacA* alleles revealed a natural double crossover m1m2/chimera. By use of a previously described expression system, each of these alleles was fused with the GST gene, respectively, and expressed as a soluble GST−VacA fusion. Despite the fact that the fusion could not form an oligomer normally found for the toxin, the recombinant VacA portion without the GST-tag indeed assembled into higher ordered structures and possessed binding activity similar to that of the native VacA. With this fusion that was locked into a predominantly monomeric state, we showed that binding level and vacuolating activity had a positive correlation, in which m1 > m1m2 > m2 in HeLa cells and there were more comparable activities in RK13 cells. Furthermore, kinetic, Scatchard, and inhibition analyses suggest the presence of at least two receptors, *RM1* and *RMX*. *RM1* is highly specific to the m1-type VacA and has a K_d of about 5 nM. Moreover, the m1-type N-terminal half midregion of VacA is crucial for *RM1* specificity. On the other hand, *RMX* interacts similarly with m1, m1m2, and m2 via a lower affinity (K_d of about 45−67 nM). The expression of mainly *RM1* on HeLa cells whereas both *RM1* and *RMX* on RK13 cells may confer distinct binding activity and therefore different cell-type specificity.

REFERENCES

1. Warren, J. R., and Marshall, B. J. (1983) *Lancet 1*, 1273−1275.
2. Parsonnet, J., Hansen, S., Rodriguez, L., Gelb, A., Warnke, A., Jellum, E., Orentreich, N., Vogelman, J., and Freidman, G. (1994) *N. Engl. J. Med. 330*, 1267−1271.
3. Blaser, M. J. (1995) *Aliment. Pharmacol. Ther. 9*, 27−30.
4. Blaser, M. J., Perez-Perez, G. I., Kleanthous, H., Cover, T. L., Peek, R. M., Chyou, P. H., Stemmermann, G. N., and Nomura, A. (1995) *Cancer Res. 55*, 2111−2115.
5. Leunk, R. D., Johnson, P. T., David, B. C., Kraft, W. G., and Morgan, D. R. (1988) *J. Med. Microbiol. 26*, 93−99.
6. Cover, T. L. (1996) *Mol. Microbiol. 20*, 241−246.
7. de Bernard, M., Aricò, B., Papini, E., Rizzuto, R., Grandi, G., Rappuoli, R., and Montecucco, C. (1997) *Mol. Microbiol. 26*, 665−674.
8. Papini, E., Satin, B., Bucci, C., de Bernard, M., Telford, J. L., Manetti, R., Rappuoli, R., Zerial, M., and Montecucco, C. (1997) *EMBO J. 16*, 15−24.
9. Atherton, J. C., Cao, P., Peek, J. R. M., Tummuru, M. K. R., Blaser, M. J., and Cover, T. L. (1995) *J. Biol. Chem. 270*, 17771−17777.
10. Marchetti, M., Aricò, B., Burroni, D., Figura, N., Rappuoli, R., and Ghiara, P. (1995) *Science 267*, 1655−1658.
11. Telford, J. L., Ghiara, P., Dell'Orco, M., Comanducci, M., Burroni, D., Bugnoli, M., Tecce, M. F., Censini, S., Covacci, A., Xiang, Z., Papini, E., Montecucco, C., Parente, L., and Rappuoli, R. (1994) *J. Exp. Med. 179*, 1653−1658.
12. Schatz, P. J., and Beckwith, J. (1990) *Annu. Rev. Genet. 24*, 215−248.
13. Schmitt, W., and Haas, R. (1994) *Mol. Microbiol. 12*, 307−319.
14. Wang, H. J., Chang, P. C. L., Kuo, C. H., Tzeng, C. S., and Wang, W. C. (1998) *Biochem. Biophys. Res. Commun. 250*, 397−402.
15. Cover, T. L., Tummuru, M. K. R., Cao, P., Thompson, S. A., and Blaser, M. J. (1994) *J. Biol. Chem. 269*, 10566−10573.
16. Phadnis, S. H., Ilver, D., Janzon, L., Normark, S., and Westblom, T. U. (1994) *Infect. Immun. 62*, 1557−1565.
17. de Bernard, M., Papini, E., de Filippis, V., Gottardi, E., Telford, J. L., Manetti, R., Fontana, A., Rappuoli, R., and Montecucco, C. (1995) *J. Biol. Chem. 270*, 23937−23940.
18. Cover, T. L., Hanson, P. I., and Heuser, J. E. (1997) *J. Cell Biol. 138*, 759−769.
19. van Doorn, L. J., Figueiredo, C., Mégraud, F., Pena, S., Midolo, P., de Magalhães Queiroz, D. M., Carneiro, F., Vanderborght, B., da Glória, F. Pegado, M., Sanna, R., de Boer, W., Schneeberger, P. M., Correa, P., Ng, E. K. W., Atherton, J., Blaser, M. J., and Quint, W. G. V. (1999) *Gastroenterology 116*, 823−830.
20. Ito, Y., Azuma, T., Ito, S., Miyaji, H., Hirai, M., Yamazaki, Y., Sato, F., Kato, T., Kohli, Y., and Kuriyama, M. (1997) *J. Clin. Microbiol. 35*, 1710−1714.
21. Wang, H. J., Kuo, C. H., Yeh, A. A. M., Chang, P. C. L., and Wang, W. C. (1998) *J. Infect. Dis. 178*, 207−212.
22. Pan, Z. J., Berg, D. E., van der Hulst, R. W., Su, W. W., Raudonikiene, A., Xiao, S. D., Dankert, J., Tytgat, G. N., and van der Ende, A. (1998) *J. Infect. Dis. 178*, 220−226.
23. Montecucco, C., Papini, E., and Schiavo, G. (1994) *FEBS Lett. 346*, 92−98.
24. Ye, D., Willhite, D. C., and Blanke, S. R. (1999) *J. Biol. Chem. 274*, 9277−9282.
25. de Bernard, M., Burroni, D., Papini, E., Rappuoli, R., Telford, J. L., and Montecucco, C. (1998) *Infect. Immun. 66*, 6014−6016.
26. de Bernard, M., Moschioni, M., Napolitani, G., Rappuoli, R., and Montecucco, C. (2000) *EMBO J. 19*, 48−56.
27. Tombola, F., Carlesso, C., Szabò, I., de Bernard, M., Reyrat, J. M., Telford, J. L., Rappuoli, R., Montecucco, C., Papini, E., and Zoratti, M. (1999) *Biophys. J. 76*, 1401−1409.
28. Szabò, I., Brutsche, S., Tombola, F., Moschioni, M., Satin, B., Telford, J. L., Rappuoli, R., Montecucco, C., Papini, E., and Zoratti, M. (1999) *EMBO J. 18*, 5517−5527.
29. Czajkowsky, D. M., Iwamoto, H., Cover, T. L., and Shao, Z. (1999) *Proc. Natl. Acad. Sci. U.S.A. 96*, 2001−2006.
30. Garner, J. A., and Cover, T. L. (1996) *Infect. Immun.*, 4197−4203.
31. Reyrat, J.-M., Lanzavecchia, S., Lupetti, P., de Bernard, M., Pagliaccia, C., Pelicic, V., Charrel, M., Ulivieri, C., Norais, N., Ji, X., Cabiaux, V., Papini, E., Rappuoli, R., and Telford, J. L. (1999) *J. Mol. Biol. 290*, 459−470.
32. Pagliaccia, C., de Bernard, M., Lupetti, P., Ji, X., Burroni, D., Cover, T. L., Papini, E., Rappuoli, R., Telford, J. L., and Reyrat, J.-M. (1998) *Proc. Natl. Acad. Sci. U.S.A. 95*, 10212−10217.
33. Massari, P., Manetti, R., Burroni, D., Nuti, S., Norais, N., Rappuoli, R., and Telford, J. L. (1998) *Infect. Immun. 66*, 3981−3984.
34. Yahiro, K., Niidome, T., Hatakeyama, T., Aoyagi, H., Kurazono, H., Padilla, P. I., Wada, A., and Hirayama, T. (1997) *Biochem. Biophys. Res. Commun. 238*, 629−632.
35. Yahiro, K., Niidome, T., Kimura, M., Hatakeyama, T., Aoyagi, H., Kurazono, H., Imagawa, K.-i., Wada, A., Moss, J., and Hirayama, T. (1999) *J. Biol. Chem. 274*, 36693−36699.
36. Seto, K., Hayashi-Kuwabara, Y., Yoneta, T., Suda, H., and Tamaki, H. (1998) *FEBS Lett. 431*, 347−350.
37. Manetti, R., Massari, P., Burroni, D., de Bernard, M., Marchini, A., Olivieri, R., Papini, E., Montecucco, C., Rappuoli, R., and Telford, J. L. (1995) *Infect. Immun. 63*, 4476−4480.
38. Wang, H. J., and Wang, W. C. (2000) *Biochem. Biophys. Res. Commun. 278*, 449−454.
39. Kuo, C. H., Poon, S. K., Su, Y. C., Su, R., Chang, C. S., and Wang, W. C. (1999) *J. Infect. Dis. 180*, 2064−2068.

40. Sambrook, J., Fritsch, E. F., and Maniatis, T. (1989) *Molecular Cloning: A Laboratory Manual*, 2nd ed., Cold Spring Harbor Laboratory Press, Cold Spring Harbor, NY.
41. Yang, J. C., Wang, T. H., Wang, H. J., Kuo, C. H., Wang, J. T., and Wang, W. C. (1997) *Am. J. Gastroenterol. 92*, 1316−1321.
42. Cover, T. L., and Blaser, M. J. (1992) *J. Biol. Chem. 267*, 10570−10575.
43. Cover, T. L., Puryear, W., Pérez-Pérez, G. I., and Blaser, M. J. (1991) *Infect. Immun. 59*, 1264−1270.
44. Ji, X., Fernandez, T., Burroni, D., Pagliaccia, C., Atherton, J. C., Reyrat, J.-M., Rappuoli, R., and Telford, J. L. (2000) *Infect. Immun. 68*, 3754−3757.
45. McClain, M. S., Schraw, W., Ricci, V., Boquet, P., and Cover, T. L. (2000) *Mol. Microbiol. 37*, 433−442.
46. Ricci, V., Galmiche, A., Doye, A., Necchi, V., Solcia, E., and Boquet, P. (2000) *Mol. Biol. Cell 11*, 3897−3909.
47. Reyrat, J.-M., Pelicic, V., Papini, E., Montecucco, C., Rappuoli, R., and Telford, J. L. (1999) *Mol. Microbiol. 34*, 197−204.
48. Ye, D., and Blanke, S. R. (2000) *Infect. Immun. 68*, 4354−4357.
49. Moll, G., Papini, E., Colonna, R., Burroni, D., Telford, J., Rappuoli, R., and Montecucco, C. (1995) *Eur. J. Biochem. 234*, 947−952.

BI010065U